

# Through-bond photoinduced electron transfer in a porphyrin-fullerene conjugate held by a Hamilton type hydrogen bonding motif†

Francis D'Souza,<sup>\*a</sup> Ganesh M. Venukadasula,<sup>a</sup> Ken-ichi Yamanaka,<sup>b</sup> Navaneetha K. Subbaiyan,<sup>a</sup> Melvin E. Zandler<sup>a</sup> and Osamu Ito<sup>\*c</sup>

Received 12th December 2008, Accepted 9th January 2009

First published as an Advance Article on the web 27th January 2009

DOI: 10.1039/b822362a

Control over the occurrence of through-bond electron transfer in self-assembled donor–acceptor conjugates is often difficult, since through-space electron transfer also competes due to the flexible nature of the spacer used to link the entities. In the present study, we have constructed a self-assembled donor–acceptor conjugate held solely by complementary hydrogen bonding and established through-bond electron transfer. The protocol used here is a Hamilton type hydrogen bonding motif involving self-assembly of a carboxylic acid functionalized porphyrin and 2-aminopyridine functionalized fullerene. Owing to the presence of two-point hydrogen bonds, the structure of the dyad is free from rotation with a donor–acceptor distance positioned appropriately to justify the through-bond electron transfer. Detailed spectral, computational and photochemical studies reveal efficient photoinduced charge separation and slow charge recombination in the studied conjugate, thus, bringing out the fundamental advantages of the directional hydrogen-bonding in the construction of donor–acceptor conjugates based on biomimetic principles and their functional role in governing electron transfer events.

## Introduction

Hydrogen bonded donor–acceptor conjugates have emerged as a standard for biomimetic model systems, as they provide a means of understanding and controlling the role of hydrogen-bonding networks in the self-assembly process and as active functioning motifs such as mediating through-bond electron transfer events.<sup>1</sup> Ground-breaking works performed by Sessler *et al.*,<sup>2</sup> De Rege *et al.*,<sup>3</sup> and more recently by Sánchez *et al.*,<sup>4</sup> and Wessendorf *et al.*,<sup>5</sup> have demonstrated that the electronic communication through hydrogen-bonding interfaces is more efficient than those found in comparable  $\sigma$ - or  $\pi$ -bonding networks. Consequently, several parallel studies aiming to further our understanding of hydrogen bonding in donor–acceptor conjugates and the resulting electron transfer in them have been reported.<sup>6–10</sup> Studies on photoinduced electron transfer in donor–acceptor conjugates are important in technological developments including organic photovoltaics and molecular electronics.<sup>1,10</sup>

The role of fullerene as an ultimate three dimensional electron acceptor in the construction of novel artificial photosynthetic models is irrefutable.<sup>11</sup> Although a combination of the characteristic selectivity and directionality of hydrogen bonds with an efficient electron-transfer process through a self-assembly directed framework is expected to advance the research field, especially in

terms of achieving longer-lived radical-ion-pair states, such studies with well-defined hydrogen bonding motifs have been limited in number.<sup>1,4,e</sup> Moreover, it has been difficult to establish occurrence of just through-bond electron transfer in contrast to through-space electron transfer due to the flexible nature of the spacer and assembled entities. In the majority of the reported donor–acceptor conjugates, through-bond and through-space electron transfer occur competitively to contribute to the fluorescence quenching mechanism.<sup>6–10</sup> In an effort to construct a self-assembled donor–acceptor conjugate held exclusively by complementary hydrogen bonding and to establish through-bond electron transfer; in the present study we have adopted a Hamilton type binding approach<sup>12</sup> involving a carboxylic acid functionalized donor and a 2-aminopyridine functionalized acceptor as a hydrogen bonding motif (Fig. 1). Owing to the presence of two-point hydrogen bonds the structure of the dyad is free from rotation with a donor–acceptor distance positioned appropriately to justify the through-bond electron transfer.

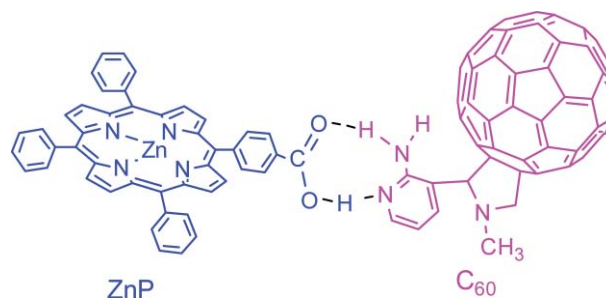


**Fig. 1** Structure of the porphyrin-fullerene conjugate held by a Hamilton type hydrogen bonding motif.

<sup>a</sup>Department of Chemistry, Wichita State University, Wichita, KS 67260-0051, USA. E-mail: Francis.DSouza@wichita.edu

<sup>b</sup>Toyota Central R & D Labs., Inc., Nagakute, Aichi, 480-1192, Japan

<sup>c</sup>Institute of Multidisciplinary Research for Advanced Materials, Tohoku University, Katahira, Sendai, Japan

† Electronic supplementary information (ESI) available: NMR titration figure, UV-vis titrations involving ZnTPP and fullerene derivative, and Stern–Volmer plots of fluorescence quenching. See DOI: 10.1039/b822362a

## Results and discussion

The synthesis of the carboxylic acid functionalized zinc porphyrin (abbreviated as ZnP in Fig. 1) was accomplished using literature methods, while the 2-aminopyridine functionalized fullerene derivative (abbreviated as C<sub>60</sub> in Fig. 1) was newly synthesized by reacting 2-amino-3-pyridylaldehyde, sarcosine and fullerene according to standard Prato synthesis of fulleropyrrolidine<sup>13</sup> (see Experimental section for details). Direct mixing of both components in *o*-dichlorobenzene yielded the target conjugate shown in Fig. 1. The complex formation was initially monitored by <sup>1</sup>H NMR spectroscopy in CDCl<sub>3</sub>. The protons corresponding to the aminopyridinyl entity revealed a slight shielding effect upon binding to the carboxyl acid group of the donor porphyrin (see ESI,† Fig. S1 for NMR figure). Importantly, none of the proton signals of the fulleropyrrolidine entity revealed significant shielding suggesting them to be sufficiently far from experiencing porphyrin ring current effects. Accordingly, the protons of the porphyrin macrocycle revealed no appreciable changes in their peak positions.

### Optical absorption and emission studies

Further details on the formation of the supramolecular complex were obtained from optical absorption and emission studies, in which variable amounts of the fullerene derivative were titrated with ZnP in *o*-dichlorobenzene as shown in Fig. 2. The absorption spectrum of the final complex was close to that obtained by the digital addition of the spectrum of individual ZnP and C<sub>60</sub> entities (both peak position and peak intensity) suggesting a lack of direct  $\pi$ - $\pi$  type interactions between the entities. The carboxylic acid–amino pyridine interactions could not be observed due to strong absorbance of the ZnP and C<sub>60</sub> entities in the UV-visible region. Control experiments performed using zinc tetraphenylporphyrin (ZnTPP) without the carboxyl functionality and 2-aminopyridine fulleropyrrolidine revealed absence of axial coordination (either

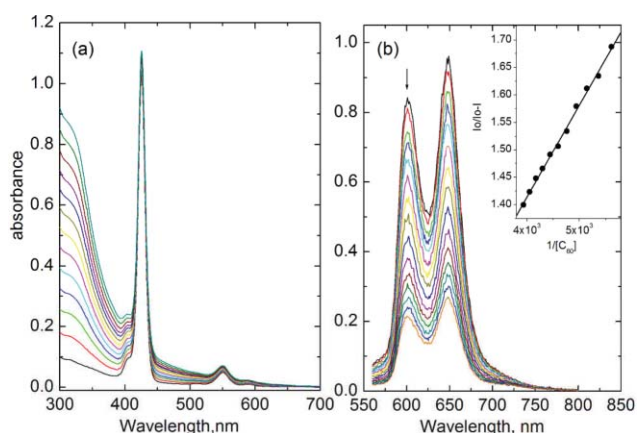


**Fig. 2** (a) Optical absorption spectrum of carboxylic acid appended zinc porphyrin (ZnP entity; 2  $\mu$ M) on increasing addition of 2-aminopyridine appended fulleropyrrolidine (C<sub>60</sub> entity; 2.6  $\mu$ M each addition) in *o*-dichlorobenzene. (b) Fluorescence emission spectrum of ZnP entity (2  $\mu$ M) on increasing addition of C<sub>60</sub> entity (2.6  $\mu$ M each addition) in *o*-dichlorobenzene.  $\lambda_{\text{ex}} = 550$  nm. The absorption band arising at 320 nm in (a) is ascribed to the C<sub>60</sub> entity. The figure inset in (b) shows a Benesi–Hildebrand plot constructed to obtain the binding constant.

*via* the pyridine or amino groups), that is, no red shifted absorption bands accompanied by isosbestic points were observed (see ESI,† Fig. S2 for optical spectra). These observations along with the NMR results rule out axial coordination as one of the binding modes in the ZnP-C<sub>60</sub> conjugate.

Interestingly, the fluorescence spectrum of the ZnP entity revealed quenching upon addition of the C<sub>60</sub> entity (Fig. 2b). Slopes of Stern–Volmer plots constructed for fluorescence quenching was found to be nearly an order of magnitude higher than that observed for the bimolecular quenching involving the ZnP entity and 2-phenyl fulleropyrrolidine (lacking the 2-aminopyridine H-bonding site) indicating the occurrence of an intramolecular quenching process in the newly formed ZnP-C<sub>60</sub> conjugate (see ESI,† Fig. S3 for Stern–Volmer plots). Additionally, the position of the emission peaks did not show any changes in the concentration range of 10<sup>-4</sup>–10<sup>-6</sup> M confirming lack of direct interaction between the ZnP and C<sub>60</sub> entities. The quenching data were analyzed according to the Benesi–Hildebrand method<sup>14</sup> to evaluate the binding constant (*K*). A binding constant of 4.4  $\times 10^3$  M<sup>-1</sup> in *o*-dichlorobenzene was obtained indicating weak-to-moderate stability of the supramolecular conjugate. This binding constant was found to be smaller than that reported for axial coordination (*K*  $\sim 10^4$  M<sup>-1</sup>)<sup>6</sup> or carboxyl-aminidinium hydrogen bonding (*K*  $\sim 10^7$  M<sup>-1</sup>) motif.<sup>4</sup> A plot using the method of continuous variation confirmed 1 : 1 stoichiometry of the conjugate.

### Computational studies

To evaluate the geometry and electronic structure of the supramolecular conjugate, DFT calculations using the B3LYP/6-31G\* method<sup>15</sup> were performed. For this, first, the ZnP and C<sub>60</sub> entities were optimized and were then allowed to interact until a stable, optimized structure on the Born–Oppenheimer potential energy surface was achieved. Fig. 3 shows the optimized geometric and electronic structures, while Fig. 4 shows the structural details of the interacting phenyl carboxylic acid and 2-aminopyridine segments of the conjugate.

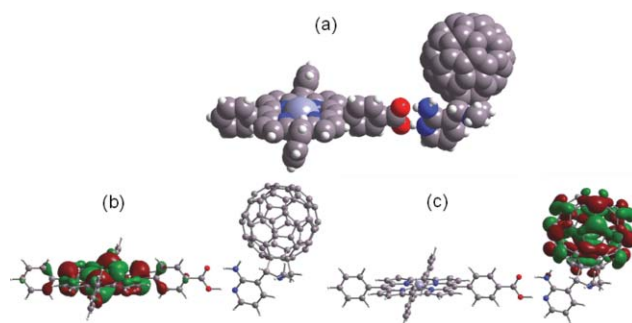


**Fig. 3** (a) B3LYP/6-31G\* optimized structure, (b) HOMO and (c) LUMO of the supramolecular ZnP-C<sub>60</sub> complex assembled *via* a Hamilton type hydrogen bonding motif.

The presence of directional H-bonding in the conjugate was supported from these optimized geometry parameters. In the optimized structure, the distance between the carboxylic acid proton and pyridine nitrogen was 1.71 Å, while the distance between the amine hydrogen and carbonyl oxygen was 1.95 Å (Fig. 4) indicating existence of H-bonding interactions. The association energy calculated with the B3LYP/6-31G\* method

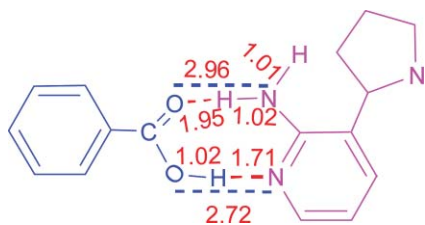


**Fig. 4** B3LYP/6-31G\* optimized geometry parameters for the carboxylic acid and 2-aminopyridine segments of the ZnP-C<sub>60</sub> conjugate in Fig. 1. The distances are given in Å.

was found to be 16.74 kcal mol<sup>-1</sup>, suggesting moderately stable complex formation. The HOMO (Fig. 3b) was fully localized on the porphyrin part while the LUMO (Fig. 3c) was localized on the fullerene part. No orbital coefficient was found on the H-bonding segment, suggesting it to be redox neutral, that is, not being part of the primary electron donating or accepting entity of the supramolecule. Thus, it is predicted that the radical cation is localized on the porphyrin unit and the radical anion is localized on the fullerene entity in the charge-separated state (ZnP<sup>•+</sup>/C<sub>60</sub><sup>•-</sup>). The center-to-center distance between the zinc porphyrin and fullerene was found to be 19.6 Å, suggesting the donor and acceptor are too distant to advance through-space electron transfer, but being possible of through-bond electron transfer. Since the ZnP and C<sub>60</sub> entities are in the same plane, orientational through-space electron transfer is also not feasible.

#### Cyclic voltammetry and free-energy changes

The redox features of the ZnP-C<sub>60</sub> conjugate were determined by cyclic voltammetry at room temperature. The voltammogram of the ZnP entity revealed reversible oxidation and reduction processes (Fig. 5). The first oxidation and reduction processes were located at  $E_{1/2} = 0.31$  and  $-1.90$  V vs. Fc/Fc<sup>+</sup>, respectively, in *o*-dichlorobenzene. Upon forming the complex by the addition of the C<sub>60</sub> entity, additional processes corresponding to the reduction of the C<sub>60</sub> entity were also observed. The first reversible reduction of the C<sub>60</sub> entity was located at  $E_{1/2} = -1.10$  V vs. Fc/Fc<sup>+</sup> while the ZnP oxidation experienced a small cathodic shift of less than 20 mV. The driving force for charge separation ( $-\Delta G_{CS}$ ) via the singlet excited state of zinc porphyrin (lowest transition energy of 2.05 eV) calculated according to the Rehm and Weller<sup>16</sup> expression was found to be  $-0.66$  eV in *o*-dichlorobenzene, indicating

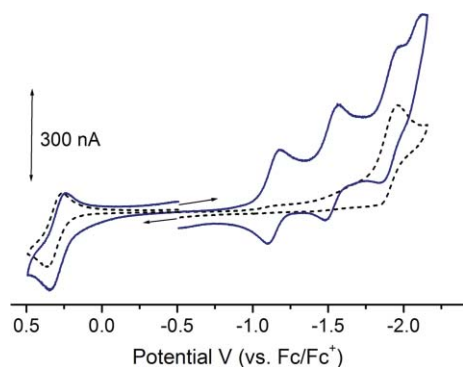


**Fig. 5** Cyclic voltammograms of ZnP entity (dotted) and ZnP-C<sub>60</sub> supramolecule (solid; blue) in *o*-dichlorobenzene, 0.1 M (*n*-C<sub>4</sub>H<sub>9</sub>)<sub>4</sub>NCIO<sub>4</sub>. Arrows show the direction of scan. Scan rate = 0.1 V s<sup>-1</sup>.

that an exothermic charge separation process is possible in the supramolecular conjugate via the <sup>1</sup>ZnP\* entity. Similarly, the free-energy change for charge recombination ( $-\Delta G_{CR}$ ) of ZnP<sup>•+</sup>/C<sub>60</sub><sup>•-</sup> was found to be  $-1.39$  eV, from which a slow charge recombination is predicted from Marcus theory due to the expected inverted region.<sup>17</sup>

#### Time resolved emission and transient absorption studies

Finally, time-resolved emission and nanosecond transient absorption studies were performed to monitor kinetics of forward and reverse electron transfer. The emission time-profile of the ZnP entity revealed a mono-exponential decay with a lifetime of 1.86 ns. Upon complexing with the C<sub>60</sub> entity, the ZnP emission revealed a bi-exponential decay with a short-lived component (0.6–0.8 ns with 20–30% fraction) and a long-lived component (1.8–1.9 ns with 70–80% fraction), in which the fractions of the short-lived component slightly increased with increasing addition of the C<sub>60</sub> entity. These fractions are in good agreement with the equilibrium concentration of the ZnP-C<sub>60</sub> conjugate calculated from the binding constant and added component concentrations. The absence of fluorescence emission of the C<sub>60</sub> entity in the 700–750 nm region in the donor-acceptor conjugate was suggestive of absence of energy transfer from the <sup>1</sup>ZnP\* to C<sub>60</sub> entity. Thus, the ZnP quenching in the dyad can be predominantly ascribed to the charge separation, whose rate constant,  $k_{CS}$  was calculated using the short lifetime according to the usual procedure adopted for intramolecular charge separation.<sup>18</sup> The value of  $k_{CS}$  thus calculated was found to be  $1.4 \times 10^9$  s<sup>-1</sup>.

The nanosecond transient absorption spectra shown in Fig. 6a revealed transient features corresponding mainly to the triplet of ZnP and C<sub>60</sub> entities in the 580–900 nm spectral region.<sup>19</sup> The triplet spectra mainly emerged from the excess of unbound components (about 70%). In addition, the characteristic peak of the C<sub>60</sub> anion radical was also observed around 1000 nm, although it was overlapped with the strong triplet absorption tails. The time profiles monitored at different wavelengths in Fig. 6b clearly show endurance of the absorption band at 1000 nm even after the decay of the triplet peaks, supporting the presence of C<sub>60</sub><sup>•-</sup>. The absorption of ZnP<sup>•+</sup>, expected to be around 600 nm, was overlapped with the triplet spectra, showing only a small shoulder. The rate constant of charge recombination,  $k_{CR}$ , can be evaluated usually by monitoring the decay of the fullerene anion radical peak at 1000 nm;<sup>18</sup> however, the overlap with triplet bands makes it difficult to explicitly measure the rate constant. Under these conditions, the absorption tail of the 1000 nm band extending to

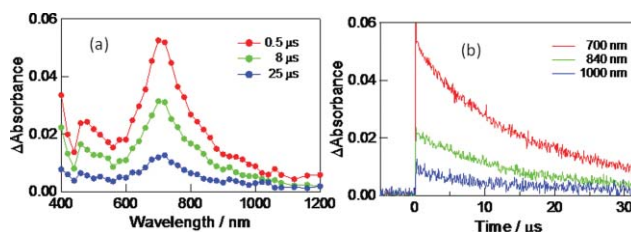


**Fig. 6** (a) Nanosecond transient absorption spectra of the ZnP-C<sub>60</sub> conjugate ( $64 \pm 5 \mu\text{M}$ ) in *o*-dichlorobenzene observed by the 425 nm laser light exposure. (b) Decay of the transients monitored at the indicated wavelengths.

the 20–30  $\mu$ s time range suggests a relatively long lived radical-ion-pair. These results suggest efficient charge separation and relatively slow charge recombination in the studied H-bonded supramolecular conjugate.

## Conclusions

In summary, by using a Hamilton type hydrogen bonding motif involving 2-aminopyridine binding to carboxylic acid, a porphyrin-fullerene conjugate has been constructed. The present donor–acceptor conjugate is held exclusively by directional hydrogen bonds as revealed by spectral and computational studies. Kinetics studies involving time-resolved emission and transient absorption studies revealed efficient photoinduced charge separation and slow charge recombination. These findings reveal the importance of the employed hydrogen bonding motif coupled with the light-harvesting porphyrin and superior electron acceptor properties of fullerene. The present study brings out the fundamental advantages of the directional hydrogen-bonding in the construction of donor–acceptor conjugates based on biomimetic principles and their functional role in governing electron transfer events.

## Experimental

### Chemicals

Buckminsterfullerene, C<sub>60</sub> (+99.95%) was from SES Research (Houston, TX). *o*-Dichlorobenzene in a sure-seal bottle, sarcosine and 2-amino-3-pyridine carboxaldehyde were from Aldrich Chemicals (Milwaukee, WI). Tetra-*n*-butylammonium perchlorate, (n-C<sub>4</sub>H<sub>9</sub>)<sub>4</sub>NClO<sub>4</sub>, was from Fluka Chemicals. All the chromatographic materials and solvents were procured from Fisher Scientific and were used as received. Synthesis and purification of the carboxyl group appended zinc porphyrin were carried out according to the literature procedures.<sup>3</sup>

### Synthesis of 2-aminopyridine appended fulleropyrrolidine

To a 150 ml toluene containing 147 mg of C<sub>60</sub>, 73 mg of sarcosine and 50 mg of 2-amino-3-pyridine carboxaldehyde was added, and the solution was refluxed for 18 h. The solvent was removed under vacuum and the product was adsorbed on silica gel. The product was purified on a silica gel column using 20 : 80 v/v ethyl acetate : toluene eluent. Yield: 60%. <sup>1</sup>H NMR (CDCl<sub>3</sub>:CS<sub>2</sub> 1 : 1 v/v  $\delta$  ppm): 8.05 (d, 1.98 Hz, 1H), 7.70 (d, 2.0 Hz, 1H), 6.62 (m, 1H), 5.01 (d, 9.6 Hz, 1H), 4.91 (s, 1H), 4.20 (d, 9.7 Hz, 1H), 2.90 (s, 3H). <sup>13</sup>C NMR (CDCl<sub>3</sub> : CS<sub>2</sub> 1 : 1 v/v  $\delta$  ppm): 39.66, 70.06, 71.09, 101.01, 136.4, 139.4, 140.3, 141.6, 142.6, 142.7, 143.2, 144.6, 144.8, 145.3, 146.1, 146.3, 148.5, 153.8, 157.3, 158.7. ESI mass in CH<sub>2</sub>Cl<sub>2</sub>, *m/z* calcd: 869.8; found: 870.0.

### Instrumentation

The UV-visible spectral measurements were carried out with a Shimadzu Model 1600 UV-visible spectrophotometer. The fluorescence emission was monitored by using a Varian Eclipse spectrometer. A right angle detection method was used. The <sup>1</sup>H NMR studies were carried out on a Varian 400 MHz spectrometer. Tetramethylsilane (TMS) was used as an internal standard. Cyclic voltammograms were recorded on an EG & G Model 263A

potentiostat using a three electrode system. A platinum button electrode was used as the working electrode. A platinum wire served as the counter electrode and a Ag/AgCl electrode was used as the reference electrode. Ferrocene/ferrocenium redox couple was used as an internal standard. All the solutions were purged prior to electrochemical and spectral measurements using argon gas.

The computational calculations were performed by DFT B3LYP/6–31G\* method with GAUSSIAN 03<sup>19</sup> software package on a high speed computer. The graphics of HOMO and LUMO coefficients were generated with the help of *GaussView* software. The ESI-Mass spectral analyses of the newly synthesized compounds were performed by using a Fennigan LCQ-Deca mass spectrometer. For this, the compounds (about 0.1 mM concentration) were prepared in CH<sub>2</sub>Cl<sub>2</sub>, freshly distilled over calcium hydride.

### Time-resolved emission and transient absorption measurements

The picosecond time-resolved fluorescence spectra were measured using an argon-ion pumped Ti:sapphire laser (Tsunami; pulse width = 2 ps) and a streak scope (Hamamatsu Photonics; response time = 10 ps). The details of the experimental setup are described elsewhere.<sup>20</sup> Nanosecond transient absorption spectra were measured by using 425 nm laser light from an OPO output (Continuum, Surelite OPO) pumped by Nd<sup>3+</sup>:YAG laser (Continuum, NY-81) as an excitation source. A 150 W xenon lamp (Hamamatsu Photonics, L2274) was used as a probe light source and incident perpendicular to the excitation light pass. The Si-APD and InGaAs-APD module (Hamamatsu Photonics, C5460) attached to a monochromator (Ritsu, MC-10N) was employed as a detector in the visible region (400–920 nm) and near-IR region (940–1400 nm), respectively. The signal from the detector was recorded on a digital oscilloscope (Tektronix, TDS3032B).<sup>21</sup> All measurements were carried out in 0.5 cm  $\times$  1 cm quartz cell (Daico MFG, USQ-E24) after bubbling with Ar-gas for 15 min at ambient temperature.

### Acknowledgements

The authors are thankful to the National Science Foundation (Grant 0804015 to FD) for support of this work. FD is thankful to the Royal Society of Chemistry for an International Author Travel Award.

### References

- (a) J.-M. Lehn, *Supramolecular Chemistry: Concepts and Perspectives*, VCH, Weinheim, 1995; (b) *Comprehensive Supramolecular Chemistry*, ed. J. L. Atwood, J. E. D. Davies, D. D. MacNicol and F. Vögtle, Pergamon, Oxford, 1996; (c) *Introduction of Molecular Electronics*, ed. M. C. Petty, M. R. Bryce and D. Bloor, Oxford University Press, New York, 1995; (d) L. Sánchez, N. Martin and D. M. Guldi, *Angew. Chem., Int. Ed.*, 2005, **44**, 5374; (e) R. Chitta and F. D'Souza, *J. Mater. Chem.*, 2008, **18**, 1440.
- J. L. Sessler, B. Wang and A. Harriman, *J. Am. Chem. Soc.*, 1993, **115**, 10418.
- P. J. F. De Rege, S. A. Williams and M. J. Therien, *Science*, 1995, **269**, 1409.
- L. Sánchez, M. Sierra, N. Martin, A. J. Myles, T. J. Dale, J. Rebek, Jr., W. Seitz and D. M. Guldi, *Angew. Chem., Int. Ed.*, 2006, **45**, 4637.
- F. Wessendorf, J.-F. Gnichwitz, G. H. Sarova, K. Hager, U. Hartnagel, D. M. Guldi and A. Hirsch, *J. Am. Chem. Soc.*, 2007, **129**, 16057.

- 6 (a) T. Hayashi and H. Ogoshi, *Chem. Soc. Rev.*, 1997, **26**, 355; (b) M. W. Ward, *Chem. Soc. Rev.*, 1997, **26**, 365; (c) D. M. Guldi, *Chem. Commun.*, 2000, 321; (d) M. E. El-Khouly, O. Ito, P. M. Smith and F. D'Souza, *J. Photochem. Photobiol., C*, 2004, **5**, 79; (e) F. D'Souza and O. Ito, *Coord. Chem. Rev.*, 2005, **249**, 1410; (f) H. Imahori and S. Fukuzumi, *Adv. Funct. Mater.*, 2004, **14**, 525; (g) F. D'Souza and O. Ito, in *Handbook of Organic Electronics and Photonics*, ed. H. S. Nalwa, American Scientific Publishers, Los Angeles, CA, 2008, vol. 1, ch. 13, pp. 485–521.
- 7 (a) J. L. Sessler, J. Jayawickramarajah, A. Gouloumis, T. Torres, D. M. Guldi, S. Maldonado and K. J. Stevenson, *Chem. Commun.*, 2005, 1892; (b) J. L. Sessler, J. Jayawickramarajah, A. Gouloumis, G. Torres and D. M. Guldi, *Tetrahedron*, 2006, **62**, 2123; (c) J. L. Sessler, C. M. Lawrence and J. Jayawickramarajah, *Chem. Soc. Rev.*, 2007, **36**, 314; (d) T. Torres, A. Gouloumis, D. S. Garcia, J. Jayawickramarajah, W. Seitz, D. M. Guldi and J. L. Sessler, *Chem. Commun.*, 2007, 292.
- 8 (a) R. Marczak, V. T. Hoang, K. Noworyta, M. E. Zandler, W. Kutner and F. D'Souza, *J. Mater. Chem.*, 2002, **12**, 2123; (b) F. D'Souza, S. Gadde, D.-M. S. Islam, S. Pang, A. L. Schumacher, M. E. Zandler, R. Horie, Y. Araki and O. Ito, *Chem. Commun.*, 2007, 480; (c) S. Gadde, D. M. S. Islam, C. A. Wijesinghe, N. K. Subbaiyan, M. E. Zandler, Y. Araki, O. Ito and F. D'Souza, *J. Phys. Chem. C*, 2007, **111**, 12400; (d) F. D'Souza, R. Chitta, A. S. D. Sandanayaka, N. K. Subbaiyan, L. D'Souza, Y. Araki and O. Ito, *Chem.–Eur. J.*, 2007, **13**, 8277; (e) F. D'Souza, R. Chitta, A. S. D. Sandanayaka, N. K. Subbaiyan, L. D'Souza, Y. Araki and O. Ito, *J. Am. Chem. Soc.*, 2007, **129**, 15865; (f) H. Nobukuni, Y. Shimasaki, T. Yuichi, F. Tani and Y. Naruta, *Angew. Chem., Int. Ed.*, 2007, **46**, 8975; (g) Z.-Q. Wu, X.-B. Shao, C. Li, J.-L. Hou, K. Wang and Z.-T. Li, *J. Am. Chem. Soc.*, 2005, **127**, 17460.
- 9 (a) J.-P. Sauvage and C. O.-D. Buchecker, *Molecular Catenanes, Rotaxanes and Knots*, Wiley-VCH, Weinheim, 1999; (b) D. B. Amabilino and J. F. Stoddart, *Chem. Rev.*, 1995, **95**, 2725; (c) R. Jager and F. Vogtle, *Angew. Chem., Int. Ed. Engl.*, 1997, **36**, 930.
- 10 (a) N. Watanabe, N. Kihara, Y. Furusho, T. Takata, Y. Araki and O. Ito, *Angew. Chem., Int. Ed.*, 2003, **42**, 681; (b) A. S. D. Sandanayaka, N. Watanabe, K. I. Ikeshita, Y. Araki, N. Kihara, Y. Furusho, O. Ito and T. Takata, *J. Phys. Chem. B*, 2005, **109**, 2516; (c) K. Li, D. I. Schuster, D. M. Guldi, A. Herranz and L. Echegoyen, *J. Am. Chem. Soc.*, 2004, **126**, 3388; (d) K. Li, P. J. Bracher, D. M. Guldi, A. Herranz, L. Echegoyen and D. I. Schuster, *J. Am. Chem. Soc.*, 2004, **126**, 9156; (e) Y. Liu, P. Liang, Y. Chen, Y.-M. Zhang, J.-Y. Zheng and H. Yae, *Macromolecules*, 2005, **38**, 9095; (f) S. Saha, A. H. Flood, J. F. Stoddart, S. Impellizzeri, S. Silvi, M. Venturi and A. Credi, *J. Am. Chem. Soc.*, 2007, **129**, 12159; (g) H. Sasabe, N. Kihara, Y. Furusho, K. Mizuno, A. Ogawa and T. Takata, *Org. Lett.*, 2004, **6**, 3957; (h) D. I. Schuster, K. Li, D. M. Guldi and J. Ramsey, *Org. Lett.*, 2004, **6**, 1919.
- 11 (a) H. Imahori and Y. Sakata, *Adv. Funct. Mater.*, 2004, **14**, 525; (b) P. V. Kamat, *J. Phys. Chem. C*, 2007, **111**, 2834; (c) N. Martin, L. Sánchez, M. Á. Herranz, B. Illescas and D. M. Guldi, *Acc. Chem. Res.*, 2007, **40**, 1015.
- 12 F. Garcia-Tellado, S. J. Geib, S. Goswami and A. D. Hamilton, *J. Am. Chem. Soc.*, 1991, **113**, 9265.
- 13 M. Maggini, G. Scorrano and M. Prato, *J. Am. Chem. Soc.*, 1993, **115**, 9798.
- 14 H. A. Benesi and J. H. Hildebrand, *J. Am. Chem. Soc.*, 1949, **71**, 2703.
- 15 M. E. Zandler and F. D'Souza, *C. R. Chim.*, 2006, **9**, 960.
- 16 (a) D. Rehm and A. Weller, *Isr. J. Chem.*, 1970, **7**, 259; (b) N. Mataga and H. Miyasaka, in *Electron Transfer*, ed. J. Jortner and M. Bixon, John Wiley & Sons, New York, 1999, part 2, pp. 431–496.
- 17 R. A. Marcus, *Angew. Chem., Int. Ed. Engl.*, 1993, **32**, 1111.
- 18 F. D'Souza, P. M. Smith, M. E. Zandler, A. L. McCarty, M. Itou, Y. Araki and O. Ito, *J. Am. Chem. Soc.*, 2004, **126**, 7898.
- 19 *Gaussian 03* (Revision B-04), M. J. Frisch, G. W. Trucks, H. B. Schlegel, G. E. Scuseria, M. A. Robb, J. R. Cheeseman, J. A. Montgomery, Jr., T. Vreven, K. N. Kudin, J. C. Burant, J. M. Millam, S. S. Iyengar, J. Tomasi, V. Barone, B. Mennucci, M. Cossi, G. Scalmani, N. Rega, G. A. Petersson, H. Nakatsuji, M. Hada, M. Ehara, K. Toyota, R. Fukuda, J. Hasegawa, M. Ishida, T. Nakajima, Y. Honda, O. Kitao, H. Nakai, M. Klene, X. Li, J. E. Knox, H. P. Hratchian, J. B. Cross, C. Adamo, J. Jaramillo, R. Gomperts, R. E. Stratmann, O. Yazyev, A. J. Austin, R. Cammi, C. Pomelli, J. W. Ochterski, P. Y. Ayala, K. Morokuma, G. A. Voth, P. Salvador, J. J. Dannenberg, V. G. Zakrzewski, S. Dapprich, A. D. Daniels, M. C. Strain, O. Farkas, D. K. Malick, A. D. Rabuck, K. Raghavachari, J. B. Foresman, J. V. Ortiz, Q. Cui, A. G. Baboul, S. Clifford, J. Cioslowski, B. B. Stefanov, G. Liu, A. Liashenko, P. Piskorz, I. Komaromi, R. L. Martin, D. J. Fox, T. Keith, M. A. Al-Laham, C. Y. Peng, A. Nanayakkara, M. Challacombe, P. M. W. Gill, B. Johnson, W. Chen, M. W. Wong, C. Gonzalez and J. A. Pople, *Gaussian, Inc.*, Pittsburgh PA, 2003.
- 20 (a) K. Matsumoto, M. Fujitsuka, T. Sato, S. Onodera and O. Ito, *J. Phys. Chem. B*, 2000, **104**, 11632; (b) S. Komamine, M. Fujitsuka, O. Ito, K. Morikawa, K. Miyata and T. Ohno, *J. Phys. Chem. A*, 2000, **104**, 11497.
- 21 H. Kawauchi, S. Suzuki, M. Kozaki, K. Okada, D. M. S. Islam, Y. Araki, O. Ito and K. Yamanaka, *J. Phys. Chem. A*, 2008, **112**, 5878.